Journal of Molecular Structure 1245 (2021) 130977

Contents lists available at ScienceDirect

Journal of Molecular Structure

journal homepage: www.elsevier.com/locate/molstr

Synthesis and characterization of two new molten acid salts: Safe and greener alternatives to sulfuric acid for the hydrolytic conversion of 1,1,1,3-tetrachloro-3-phenylpropane to cinnamic acid

Lia Zaharani [a], Hayedeh Gorjian [b], Mohd Rafie Johan [a], Nader Ghaffari Khaligh [a,b,*]

[a] Nanotechnology and Catalysis Research Center,3rd Floor, Block A, Institute of Postgraduate Studies, University of Malaya, 50603, Kuala Lumpur, Malaysia
[b] Department of Food Science and Technology, Sari Agricultural Sciences and Natural Resources University, Sari, Iran

ARTICLE INFO

Article history:
Received 31 March 2021
Revised 22 June 2021
Accepted 23 June 2021
Available online 13 July 2021

Keywords:
Molten acid salt
Structure elucidation
Brönsted acid
Homogeneous catalysis
Cinnamic acid

ABSTRACT

Available online Two new acid salts were synthesized, and their chemical structures were characterized by various spectra data analyses. Although ^{1}H NMR did not show acid proton of $[HSO_4]^-$, the FTIR spectra of molten acid salts act as key support to approve of their chemical structures. The structure elucidation of the molten acid salts demonstrated the existence of 4,4′-trimethylene-N,N′-dipiperidinium dication with sulfate and hydrogen sulfate anion(s). Thus, sulfuric acid can act as a diprotic or monoprotic Brönsted acid when it is treated by a secondary amine regarding the initial mole ratio of sulfuric acid and amine. Also, the catalytic activity of these molten acid salts was investigated for the hydrolytic conversion of (1,3,3,3-tetrachloropropyl)benzene to cinnamic acid. The desired product was obtained in 88 ± 2.0% yield under optimal conditions. The molten acid salts were high recyclable and their chemical structure and catalytic efficiency showed no significant change even after the 5th run. Furthermore, TMDP-SA (1:1) showed a much weaker corrosive property compared with TMDP-SA (1:2) and SA (98%), and the surface of stainless steel was intact even after 24 h. This fact and the acidity of two molten acid salts also confirm the proposed chemical structures.

1. Introduction

Catalysts play a vital role in organic chemistry and synthetic processes. The synthesis and introduction of new catalysts and investigation of their catalytic efficiency are interest topics in catalysis research, along with the design of greener and eco-friendly technologies under realistic conditions regarding air atmosphere, high temperature, normal pressure, and humidity.

It is well known that the physical and chemical properties of compounds depend on the chemical structure of their constituent particles and the attraction or repulsion forces between neighboring particles, including molecules and ions. Moreover, the reaction mechanism is mainly dependent on the chemical structure and active sites [1]. Therefore, the structure elucidation of new chemicals and catalysts plays a vital role in the study and evaluation of applications and reactions, and many instrumental methods are employed to provide clues to avoid the pitfalls for future structure elucidation works [2].

Sulfuric acid (SA) has been applied as a catalyst, co-catalyst, oxidant, co-oxidant, dehydrating, and sulfonating agent in many academic and industry processes [3–5]. The treatment of most organic and inorganic bases with SA can give the $[HSO_4]^-$ or $[SO_4]^{2-}$ dependence on reactant mole ratio, the nature, and basicity of base. Free sulfate anion has Td symmetry, while the symmetry of hydrogen sulfate reduces to C3v, thus, their FTIR spectra will display their characterizing peaks in different frequencies [6–8]. The ^{1}H NMR spectra of species $[HSO_4]^-$ or $[SO_4]^{2-}$ can be similar because the proton chemical shift of $[HSO_4]^-$ cannot be often detected due to many reasons [9].

Molten salts are well-known as ionic liquids having a melting point above 100°C containing cationic nitrogen or phosphorus cores with the charge-balanced by organic or inorganic counterion. The electrostatic interactions between the cations and anions, which in turn is dependent on nature, size, and charge of cations and anions, can result in various physical and chemical properties of the molten salts. Therefore, the molten salts can be designed to achieve the appropriate physical and chemical properties. Although they were initially used as eco-friendly solvents in chemical reactions, ILs/molten salts are now employed in many fields including thermal energy storage (TES) [10], and heat transfer at relatively

* Corresponding author.
E-mail address: ngkhaligh@um.edu.my (N.G. Khaligh).

https://doi.org/10.1016/j.molstruc.2021.130977
0022-2860/

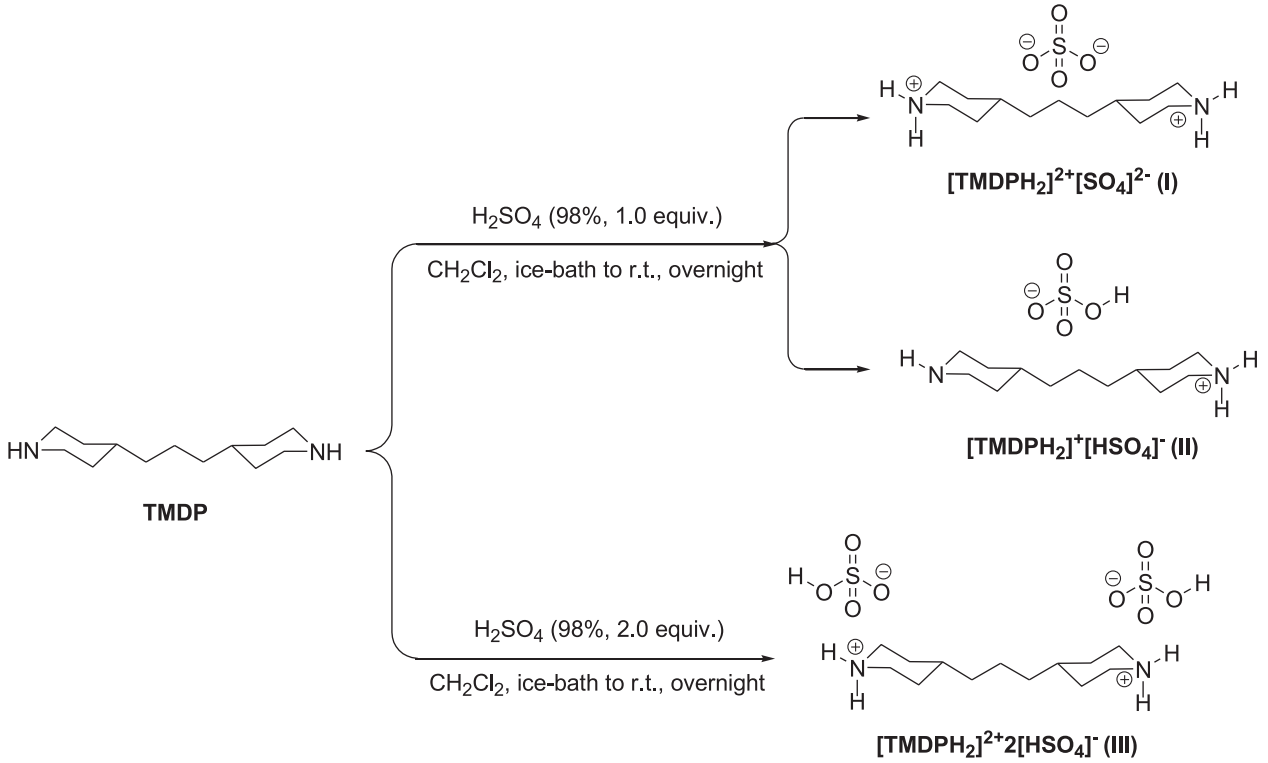

Scheme 1. The possible structures of new molten acid salts.

high temperatures due to their large capacity for heat storage [11], synthesis and catalysis [12–16].

Cinnamic acid and its derivatives play a crucial role in the complex phenolic compound formation [17]. Cinnamic acid and its derivatives have been extensively investigated in medicinal research due to its antitumor, anti-inflammatory, and anticancer [18,19], antifungal activities [20]. They have been used in the management of lipid metabolism and obesity [21]. It was found that cinnamic acids, as antioxidant phytochemicals, showed protective and/or therapeutic effects against diabetes and other diabetic disorders with high oxidative stress conditions [22]. Cinnamic acid (CA) and its hydroxy-derivatives have been extensively used in the preparation of polymers [23], cosmetics and possess various functions [24].

The Perkin reaction, the Claisen condensation, the Knoevenagel condensation, and modification of these reactions have been utilized as principal synthetic methods to prepare cinnamic acid. Cinnamic acid derivatives have also been synthesized through genetically engineered microorganisms [24]. Cinnamic acid has also been produced through the hydrolyzation of (1,3,3,3-tetrachloropropyl)benzene (TCPB) in acetic acid as a solvent and in the presence of sulfuric acid as a catalyst [25]. Many molten salts/ionic liquids, bearing an alkane sulfonic acid moiety in an imidazole, triphenylphosphine, pyridinium cation, and imidazolium or pyridinium cation and hydrogen sulfate counteranion, have been applied as dual solvent-catalysts in the different organic reactions, including selective oxidation [26], alkylation reaction [27], Fischer esterification, transesterification, alcohol dehydrodimerization, and the pinacol/benzopinacole rearrangement [28–30], and synthesis of Chalcone [31]. The quaternary ammonium ionic liquids such as $[Et_3NH][HSO_4]$ have been reported as dual solvent-catalysts for the preparation of cinnamic acid through the hydrolytic reaction of TCPB [32].

In continuing our previous works on 4,4′-trimethylenedipiperidine (TMDP) [33–35] and the synthesis and catalytic application of molten salts [36], ionic liquids having a melting point above 100 °C, the synthesis of two new acid salts was designed and carried out through stirring 4,4′-trimethylenedipiperidine (TMDP) and sulfuric acid (98%) in CH_2Cl_2. The new molten acid salts were characterized by spectroscopic techniques. The presence of different anions, including sulfate and hydrogen sulfate, was demonstrated by complementary analysis of FTIR, pH, melting point, and solubility. The physical properties of the new acid salts were determined and recorded. Then, the catalytic activity of new molten acid salts was demonstrated for the direct synthesize of cinnamic acid through hydrolyzation of (1,3,3,3-tetrachloropropyl)benzene (TCPB) under obtained optimal reaction conditions. The acid salts and cinnamic acid were easily separated by simple filtration. After concentrating the aqueous solution of acid salts, after concentrating, they were reused in subsequent runs with a slight loss of catalytic efficiency after the 5^{th} run. A study of corrosive property showed that TMDP-SA (1:1) is a much weaker corrosive compared with TMDP-SA (1:2), which in turn is weaker corrosion than SA (98%). This fact can be counted as further support for the proposed chemical structures.

2. Results and discussion

2.1. Synthesis and the structure elucidation of new acid salts

The treatment of the commercially available TMDP with sulfuric acid (SA) (98%) in a mole ratio of 1:1 and 1:2 can lead to three possible chemical structures of ionic salts through the acid-base reaction of TMDP, containing two piperidine rings, and sulfuric acid as a diprotic acid (Scheme 1).

The viscous pale yellow liquids were isolated after 24 h of stirring at mild conditions. The colorless clear crystals were formed from methanol.

The new molten acid salts were characterized by the detailed ^1H NMR and ^{13}C NMR and ^1H,^1H-COSY, mass spectra, and FTIR

Table 1
The NMR data of TMDP-SA(1:2) in DMSO-d_6 and D_2O.

Atom	DMSO-d_6			D_2O		
	δH (ppm)	J (Hz)	δC (ppm)	δH (ppm)	J (Hz)	δC (ppm)
NH^+(eq)	8.44	br s	-	-		-
NH^+(ax)	8.15	br s	-	-		-
C-2, 2′, 6 and 6′(eq)	3.21	d, 12.4	43.69	3.29	d, 12.8	44.15
C-2, 2′, 6 and 6′(ax)	2.80	dd, 12.1 and 23.2	43.69	2.85	td, 2.5 and 12.9	44.15
C-3, 3′, 5 and 5′(eq)	1.75	d, 13.1	28.63	1.83	d, 14.0	28.37
C-3, 3′, 5 and 5′(ax)	1.26–1.15	m	28.63	1.27-1.17	m	28.37
C-4 and 4′	1.49–1.44	m	35.71	1.53-1.46	m	34.97
C-α	1.26–1.15	m	33.02	1.27-1.17	m	32.76
C-β	1.26–1.15	m	28.63	1.27-1.17	m	22.29

spectra of the new acid salts. First, the reaction of TMDP and SA (98%) was carried out in CH_2Cl_2 at a ratio of 1:2 at room temperature overnight. The obtained pale yellow liquid was washed three times by dichloromethane. The colorless clear crystals were obtained after crystallization from methanol.

The FTIR analysis of TMDP-SA (1:1) and TMDP-SA (1:2)

The ^1H and ^{13}C NMR was recorded in DMSO-d_6 (See supplementary information, Figure S1). The equatorial hydrogens (H_{eq}) of CH-2, 2′, 6, and 6′ and their axial counterpart (H_{ax}) were exhibited as doublet and doublet-doublet at 3.21 ppm (J = 12.4 Hz) and 2.80 ppm (23.2 and 12.1 Hz). The H_{eq} and H_{ax} of CH-3, 3′, 5, and 5′ were observed as an apparent doublet and multiplet at 1.75 ppm (J = 13.1 Hz) and 1.26–1.15 ppm, respectively. The H_{ax} of CH-4 and 4′ were displayed at 1.49–1.44 ppm. The protons of trimethylene spacer appeared as a multiplet at 1.26–1.15 ppm. The ^1H NMR of TMDP-SA (1:2) in D_2O demonstrated the hydrogen exchange of protons at 8.44 and 8.15 ppm with the deuterium of heavy water acid properties (See supplementary information, Figure S2). The ^{13}C NMR of TMDP-SA (1:2) in DMSO-d_6 and D_2O displayed five different types of carbons (See supplementary information, Figure S1 and S2) (Table 1).

The correlations between peaks at 8.46 and 8.17 ppm with themselves and Heq and Hax of C2, C2′, C6, C6′ at 3.23 ppm and 2.82 ppm was observed in ^1H,^1H-COSY spectra of TMDP-SA (1:2) in DMSO-d_6, which confirm the structure of piperidinium cation (See supplementary information, Figure S3).

In order to investigate the existence of an excess of SA in the product, a given volume of SA (98%) (10.0 μL, 0.18 mmol, and 20.0 μL, 0.37 mmol) was added into the NMR tube, containing the product TMDP-SA (1:2). Then, the ^1H and ^{13}C NMR of these samples, as well as the ^1H NMR of SA (98%), were recorded (See supplementary information, Figs. S4-S6). Furthermore, to gain further understanding of the interactions between the $[TMDPH_2]^{2+}$ dication and $[SO_4]^{2-}$ and $[HSO_4]^-$ anions, we have evaluated the shift change of the proton signals of the $[TMDPH_2]^{2+}$ dication for TMDP-SA(1:2) upon the incremental addition of SA (10.0 and 20.0 μL). The protons in the $[TMDPH_2]^{2+}$ dication showed no significant shift ($\Delta\delta$ = 0.2 ppm) to a high magnetic field side upon the incremental addition of SA, while the peak of HOD significantly moved to a low field (downfield) side. These results strongly suggest that the acid pH has no notable effect on the protons of $[TMDPH_2]^{2+}$ dication. The singlet sharp peak of HOD was observed at 3.71 ppm in ^1H NMR of TMDP-SA(1:2), whereas the sharp peaks at 6.95 and 8.15 ppm appeared in the ^1H NMR of samples containing TMDP-SA(1:2) with 10.0 and 20.0 μL excess of SA (98%), respectively (See supplementary information, Figures S4 and S5). The hydrogen ions of excess of SA can be readily exchanged with the hydrogen of water, and due to the stronger intermolecular hydrogen bonding between the SA proton and water molecules, the ^1H NMR of HOD signal appears at the lower magnetic field (higher frequency) [37].

Table 2
The NMR data of TMDP-SA(1:1) with 10 μL excess of SA (98%) in DMSO-d_6.

Atom	DMSO-d_6		
	δH (ppm)	J (Hz)	δC (ppm)
NH^+(eq)	8.45	d, 9.1	-
NH^+(ax)+SA protons	8.16	s	-
C-2, 2′, 6 and 6′(eq)	3.17	d, 12.4	43.90
C-2, 2′, 6 and 6′(ax)	2.77	dd, 12.4 and 23.3	43.90
C-3, 3′, 5 and 5′(eq)	1.71	d, 13.0	28.77
C-3, 3′, 5 and 5′(ax)	1.13	dd, 7.0 and 14.4	28.77
C-4 and 4′	1.48-1.40	m	35.93
C-α	1.26-1.19	m	33.02
C-β	1.26-1.19	m	23.02

A sharp singlet at 7.13 ppm was detected for the same amount of SA (10.0 μL, 0.18 mmol) in DMSO-d_6 (See supplementary information, Figure S6). Regarding the lack of sharp or broadened peaks from 4.0 ppm to 8.0 ppm and > 9.0 ppm in the ^1H NMR spectrum of TMDP-SA(1:2), the excess SA in this acid molten salt was excluded. On the other hand, acid protons of hydrogen sulfate were not observed probably due to strong hydrogen bonding and interaction between cation and anion as well as the presence of water in DMSO-d6. The ^{13}C NMRs showed negligible shifts after adding sulfuric acid (98%).

Some important differences were observed in the comparison between the solubility of TMDP-SA(1:1) and TMDP-SA(1:2) in the deuterated solvents. Both of them easily dissolved in D_2O and methanol-d4 at room temperature. Although TMDP-SA (1:2) dissolve partially and completely at room temperature and 50 °C in DMSO-d_6, respectively; TMDP-SA(1:1) did not dissolve in DMSO-d_6 at room temperature and even 50 °C after four hours. By addition 10 μL of SA (98%) (0.18 mmol) to an NMR tube containing 50 mg of TMDP-SA(1:1) in DMSO-d6, a clear solution was obtained viz. an excess of SA causes the dissolving of TMDP-SA(1:1) in DMSO-d_6.

The ^1H and ^{13}C NMRs of TMDP-SA(1:1) in three deuterated solvents, D_2O (ε = 78.5), methanol-d_4 (ε = 32.7) and DMSO-d_6 (ε = 46.7) with significantly different dielectric constants, solvation, and hydrogen bonding ability are depicted in Figures S7-S9 (See supplementary information), and all informative NMR data are collected in Tables 2 and 3.

The chemical shift of methylene groups of TMDP-SA(1:1) in three deuterated solvents, D_2O (ε = 78.5), methanol-d_4 (ε = 32.7), and DMSO-d6 (ε = 46.7) with significantly different dielectric constants, solvation and hydrogen bonding ability data are reported in Table 2.

The results demonstrated that the methylene protons of piperidine rings of $[TMDPH_2]^{2+}$ were influenced through intermolecular hydrogen bonds by D_2O with a high dielectric constant and solvation ability. Due to the strong intermolecular hydrogen bond, the solvent molecules around the $>NH_2^+$ protons are included, leading

Table 3
The NMR data of TMDP-SA(1:1) in methanol-d_4 and D_2O.

Atom	Methanol-d_4			D_2O		
	δH (ppm)	J (Hz)	δC (ppm)	δH (ppm)	J (Hz)	δC (ppm)
NH^+(eq)	-	-	-	-	-	-
NH^+(ax)	-	-	-	-	-	-
C-2, 2′, 6 and 6′(eq)	3.38	d, 12.8	45.23	3.42	d, 12.8	44.15
C-2, 2′, 6 and 6′(ax)	2.94	td, 2.5 and 12.8	45.23	2.98	td, 3.0 and 13.0	44.15
C-3, 3′, 5 and 5′(eq)	1.89	d, 13.6	30.02	1.96	d, 14.0	28.37
C-3, 3′, 5 and 5′(ax)	1.31	dd, 6.9 and 14.5	30.02	1.32	dd, 6.7 and 14.0	28.37
C-4 and 4′	1.61–1.54	m	37.09	1.66–1.59	m	34.97
C-α	1.47–1.37	m	34.94	1.41–1.35	m	32.76
C-β	1.47–1.37	m	24.23	1.41–1.35	m	22.29

Table 4
The ^{1}H NMR data of TMDP, TMDP-SA(1:2), and TMDP-SA(1:1) + excess of SA in DMSO-d_6.

Atom	TMDP		TMDP-SA(1:2)		TMDP-SA(1:1) + SA (10 μL)	
	δH (ppm)	J (Hz)	δH (ppm)	J (Hz)	δH (ppm)	J (Hz)
NH^+(eq)	-	-	8.44	br s	8.45	d, 9.1
NH^+(ax)	-	-	8.15	br s	8.16	s (along with SA peak)
CH-2, 2′, 6 and 6′(eq)	2.86	d, 9.4	3.21	d, 12.4	3.17	d, 12.4
CH-2, 2′, 6 and 6′(ax)	2.38	dd, 10.9 and 10.4	2.80	dd, 12.1 and 23.2	2.77	dd, 12.4 and 23.3
CH-3, 3′, 5 and 5′(eq)	1.54	d, 10.4	1.75	d, 13.1	1.71	d, 13.0
CH-3, 3′, 5 and 5′(ax)	1.16–1.10	m	1.26–1.15	m	1.13	dd, 7.0 and 14.4
CH-4 and C4′	1.29–1.20	m	1.49–1.44	m	1.48–1.40	m
CH_2-α	0.98–0.91	m	1.26–1.15	m	1.26–1.19	m
CH_2-β	1.29–1.20	m	1.26–1.15	m	1.26–1.19	m

Table 5
The ^{13}C NMR data of TMDP, TMDP-SA(1:2), and TMDP-SA(1:1) + SA in DMSO-d_6.

Atom	TMDP δC (ppm)	TMDP-SA(1:2) δC (ppm)	TMDP-SA(1:1) + SA (10 μL) δC (ppm)
C-2, 2′, 6 and 6′	46.35	43.69	43.90
C-2, 2′, 6 and 6′	46.35	43.69	43.90
C-3, 3′, 5 and 5′	33.40	28.63	28.77
C-3, 3′, 5 and 5′	33.40	28.63	28.77
C-4 and 4′	37.24	35.71	35.93
C-α	36.05	33.02	33.02
C-β	22.92	28.63	23.02

to significant solvation and, thus, very large chemical shift solvent-dependence.

The resulting chemical shifts in DMSO-d_6 (δ = 3.17, 2.77, 1.71, 1.13 ppm), methanol-d_4 (δ = 3.38, 2.94, 1.89, 1.31 ppm) and D_2O (δ = 3.42, 2.98, 1.96, 1.32 ppm) indicate that hydrogen bond between the $[TMDPH_2]^{2+}$ and D_2O is more efficient than in methanol-d_4 and significantly stronger than in DMSO-d_6. This demonstrates the great sensitivity of ^{1}H NMR chemical shifts to the intermolecular hydrogen bond between $[TMDPH_2]^{2+}$ and the deuterated solvents.

The ^{1}H and ^{13}C NMR of pure TMDP was also recorded in the same deuterated solvent i.e., DMSO-d_6 (See supplementary information, Figure S10). The symmetrical equatorial and axial CH_2 groups of TMDP-SA(1:2) and TMDP-SA(1:2) + excess SA appeared at 3.21, 3.17, and 2.80, 2.77 ppm as broad doublet and doublet-doublet, respectively. They were displayed with a higher chemical shift ($\Delta\delta^1$H ~0.31–0.42 ppm) and a larger coupling constant (ΔJ ~1.5–12.4 Hz) than that of pure TMDP, probably due to the deshielding effect of $>NH_2^+$ groups and decrease of the electron density around of protons. The C-2,2′,6,6′ and C-3,3′,5,5′ chemical shifts of the TMDP-SA(1:2) and TMDP-SA(1:2) + excess SA are recorded at 43.69, 43.90 and 28.63, 28.77 ppm in DMSO-d_6, respectively; which are lower than that of TMDP ($\Delta\delta^{13}$C = 2.45–4.77 ppm), and this demonstrated the protonation of TMDP as reported in the literature [38] (Tables 4 and 5).

2.2. The FTIR analysis of TMDP-SA(1:1) and TMDP-SA(1:2)

The infrared spectra of neat TMDP, TMDP-SA(1:1), and TMDP-SA(1:2) are depicted in Fig. S11 (See supplementary information). The N–H stretch and N–H wag of piperidine rings of TMDP appears at 3396 and 3286 cm^{-1}, and 809 cm^{-1}. The sharp peaks at 1144 and 1109 cm^{-1} were assigned to C–N asymmetric stretching vibrations. The C–C bending and stretching modes of TMDP appeared as sharp peaks at 1286 and 1264 cm^{-1}, and a weak band at 1000 cm^{-1}, respectively. A strong band at 1322 cm^{-1} was attributed to methylene C–H wagging frequency. The asymmetric and symmetric C–H vibration of methylene groups next to NH_2^+ ($-CH_2-NH_2^+-CH_2-$) was observed at 2918, 2840, and 2742 cm^{-1} as the medium and sharp peaks, respectively. Also, the methylene C–H bending vibrations displayed medium intensity and relatively broad peaks at 1472 and 1425 cm^{-1}. The CCN deformation vibrations were observed at 648 and 593 cm^{-1} as medium and weak intensity peaks. The weak intensity peak at 725 cm^{-1} was assigned to the torsion of piperidine rings of TMDP [39].

As can be seen in Figure S11, the vibration N–H at $>NH_2^+$ groups of TMDP-SA(1:1) was observed as a strong intensity and sharp peak at 3431 cm^{-1}, while this stretching vibration appeared in FTIR of TMDP-SA(1:2) as a medium intensity and broad peak at 3409 cm^{-1}. The bands at the range of 2930–2859 cm^{-1} and 3035–2852 cm^{-1} were attributed to the symmetric and antisymmetric stretching vibrational of methylene groups in the piperidinium rings of TMDP-SA(1:1) and TMDP-SA(1:2), respectively. The wagging mode of methylene groups of the piperidinium rings of TMDP-SA(1:1) and TMDP-SA(1:2) was detected at 1314 and 1302 cm^{-1}, respectively. Medium intensity peaks at 2516 and 2713 cm^{-1} were assigned to the N–H stretching vibration of the piperidinium rings of TMDP-SA(1:1), and TMDP-SA(1:2) also exhibited a weak intensity band at 2526 cm^{-1} for this vibration. This bathochromic shift of N–H stretch vibration was assigned to the relative acceptor capability of H-bond acceptor capability of sulfate and hydrogen sulfate [40,41], which is in good agreement with the formation of different anions in the TMDP-SA(1:1) and TMDP-SA(1:2).

The FTIR spectrum of TMDP-SA(1:1) showed two medium intensity bands at 1624 and 1457 cm^{-1}, and these peaks were observed at 1615 and 1462 cm^{-1} for TMDP-SA(1:2). Based on the previously reported in the literature [42], the deformation vibration modes of $>NH_2^+$ groups of secondary amine salts are displayed in this range, which demonstrates the formation of piperidinium cation. TMDP-SA (1:1) showed a multi-branched strong broad peak at a range 1101–1030 cm^{-1} for the asymmetric and symmetric SO_2 stretching vibrations, while these vibrations appeared as strong intensity bands 1151 and 1032 cm^{-1} for TMDP-SA(1:2). A strong band at 858 cm^{-1} together with a weak band at 731 cm^{-1} and a strong band at 578 cm^{-1} were attributed to S–OH stretching modes and SO_2 bending of hydrogen sulfate anion. These bands are merely observed in the FTIR of TMDP-SA (1:2), while the SO_2 bending vibration of TMDP-SA(1:1) appeared at 612 cm^{-1} [43-45].

2.3. The mass spectra analysis of TMDP-SA(1:1) and TMDP-SA(1:2)

The prominent $[M+EtOH+NH_4]^+$ and $[M+EtOH+CO_2+NH_4]^+$ (where M corresponds to TMDP) were detected at m/z 274.2753 and 318.3014, respectively, in the positive ion mode of TMDP-SA(1:1) and TMDP-SA(1:2). In contrast, the negative ion mode showed a weak ion at m/z 339.2005 corresponding to $[M+H+SO_4+CH_3OH]^-$ or $[M+HSO_4+CH_3OH]^-$. The isotope distribution patterns were observed in the positive ion mode as follows: m/z (mass intensity %) 274.2753 (100.0), 275.2779 (15.2), 276.2805 (1.2) and 318.3014 (100,0), 319.3042 (17.9), 320.3065 (1.5) (See supplementary information, Fig. S12).

2.4. The physical properties of TMDP-SA(1:1) and TMDP-SA(1:2)

The total water content of TMDP-SA(1:1) and TMDP-SA(1:2) was determined 0.67 ± 0.02 wt. % and 0.21 ± 0.02 wt. % respectively, by Karl Fisher (KF) titration, using a Metrohm 831 KF coulometer in conditions of ambient humidity and room temperature. The melting point of TMDP-SA (1:2) was 110°C, while TMDP-SA (1:1) decomposed at 290 °C. The aqueous solution of TMDP-SA (1:1) and TMDP-SA (1:2) (50 mg in 25 mL of ultrapure water) displayed pH 2.03 ± 0.02 and 3.65 ± 0.02, respectively (An average of three readings). Although TMDP-SA (1:2) dissolved in dimethyl sulfoxide (DMSO) at room temperature, TMDP-SA (1:2) was insoluble in DMSO even at 50°C. TMDP-SA (1:1) and TMDP-SA (1:2) were soluble in methanol, water, acetic acid, while they did not dissolve in ethanol, chloroform, dichloromethane, ethyl acetate, acetonitrile, and n-hexane.

2.5. The titrimetry analysis of the aqueous solution of TMDPS-SA(1:2) and TMDP-SA(1:1)

Further support for the structure elucidation was obtained by a titrimetry analysis of the aqueous solution of TMDPS-SA(1:2) and TMDP-SA(1:1). One plateau is observed in the titration curve of TMDP-SA(1:2) (See supplementary information, Fig. S13). The obtained value, by considering the experimental errors, is in good agreement with the proposed chemical structure, two moles of $[HSO_4]^-$ per TMDP-SA(1:2). The titration curve of TMDP-SA(1:1) shows that only one drop was enough to neutralize the TMDP-SA(1:1), which demonstrates less acidity of this molten salt (Table 6) (See supplementary information, Figure S14).

2.6. The X-ray diffraction (XRD) pattern of TMDP-SA(1:2) and TMDP-SA(1:1)

The structure of TMDP-SA (1:1) and TMDP-SA(1:2) was also studied using an XRD pattern at a range of 2–80°. The XRD spectra approved that the new organic salts have a crystalline nature (See supplementary information, Figure S15). The average size of particles (Dp) and interplanar spacing (d) was calculated from Debye Scherrer and Bragg's equations.

Debye Scherrer equation:

$$Average\ crystallitesize\ (Dp) = (0.94 \times \lambda)/(\beta \times \mathrm{Cos}\theta)$$

Bragg's equation:

$$Interplanar\ spacing\ (d) = Order\ of\ Reflection(n) \times Wavelength(\lambda)/2 \times Sin\theta$$

Where, β = peak Full Width at Half Maximum (FWHM), θ = Bragg angle, λ = X-Ray wavelength of Cu Kα (0.15418 nm)

The results exhibited a crystallite size at a range of 36–139 nm, and the interplanar spacing (d) was at a range of 0.28–1.08 nm [46,47].

Based on the above-mentioned results, it is indicated that TMDP-SA(1:1) and TMDP-SA(1:2) can form the structures **I** ($[TMDPH_2]^{2+}[SO_4]^{2-}$) and **III** ($[TMDPH_2]^{2+}\ 2[HSO_4]^-$), respectively, through an acid-base of one or two equivalent(s) sulfuric acid with TMDP. It seems that two protons of sulfuric acid have nearly the same acidic properties in organic solvents such as CH_2Cl_2, and sulfate anion can be formed instead of hydrogen sulfate anion when TMDP reacts with sulfuric acid in a mole ratio of 1:1.

2.7. Synthesize of cinnamic acid through hydrolyzation of TCPB using TMDP-SA(1:1) and TMDP-SA(1:2) as the catalyst

The different parameters including the catalyst loading, the use of HOAc or water as solvent, temperature, and reaction time were optimized for the preparation of cinnamic acid through hydrolyzation of TCPB (Table 7). Cinnamic acid was detected in 12% yield when the reaction was conducted by using a mix of H_2SO_4 and acetic acid at 100 °C within 4 h, only 12% yield of cinnamic acid (Table 7, entry 1). Cinnamic acid was obtained in 48% and 64% yield in the presence of TMDP-SA(1:1) and TMDP-SA(1:2), respectively, at the aforementioned conditions (Table 7, entries 2 and 3). Although the higher loading of TMDP-SA(1:2) led to the better conversion of TCPB and the higher yield of cinnamic acid, this improvement could not continue when the loading of TMDP-SA(1:2) reached 20 mg or greater (Table 7, entries 3-5). Entries 6–8 in Table 7 show that the optimal temperature and reaction time are 100 °C and six hours, respectively (Table 7, entries 6-8). The same yield of cinnamic acid was obtained when the reaction was performed in the presence of TMDP-SA(1:1) (20 mg) in HOAc as a solvent instead of water (Table 7, entry 9).

The yield of the hydrolytic reaction was largely affected by the acid property and anion type of acid salts. TMDP-SA(1:2) gave a higher yield of cinnamic acid than TMDP-SA (1:1). It is worth mentioning that the hydrolyzation of TCPB could be carried out in both acid salts.

After removing the water by a rotary evaporator under a high vacuum ($< 10^{-4}$ Torr), TMDP-SA (1:2) could be recycled in four subsequent runs. Our results showed that a small amount of water in the acid salt did not affect the recycling of TMDP-SA (1:2), and the yield was not reduced after being recycled four times (Table 8).

Hydrolysis of 1,1,1,3-tetrachloro-3-phenylpropane was carried out with perchloric acid in acetic acid according to a previously reported method in the literature [48,49], which gave a 38% yield of cinnamic acid. Also, the hydrolyzation of 1,1,1,3-tetrachloro-3-phenylpropane in the presence of $[Et_3NH][HSO_4]$ as an ionic liquid, as described by Li et al., gave cinnamic acid in 63% yield [50].

Hydrolytic dehydrochlorination and dechlorination can be promoted by TMDP-SA(1:2) and TMDP-SA(1:1), containing piperdinium rings and hydrogen sulfate and sulfate anions, in an aqueous medium (Scheme 2). The process is probably involved the con-

Table 6
Some data for the titrimetry analysis of TMDP-SA(1:1) and TMDP-SA(1:2).

Entry	Acid salt	Molecular weight (g mol^{-1})	Molarity (mol L^{-1})	pH at temp. 27.5 ± 0.3
1	TMDP-SA(1:1)	308.44	6.5×10^{-3}	5.25
2	TMDP-SA(1:2)	406.51	4.9×10^{-3}	2.25

[a] Based on the proposed chemical structures.
[b] 50 mg of salt in 25 mL of deionized water.
[c] The mean of the triplicate measurements.

Table 7
The effect of different parameters on the conversion of the TCPB to cinnamic acid.[a]

Entry	Catalyst	Catalyst loading			Solvent	Temp. (°C)	Reaction time (h)	Yield (%)[b]
		mg	mmol	mol%				
1	H_2SO_4 (98%)	10	0.100	8.8	HOAc	100	4.0	12
2	TMDP-SA(1:1)	10	0.032	3.0	H_2O	100	4.0	48
3	TMDP-SA(1:2)	10	0.024	2.3	H_2O	100	4.0	64
4	TMDP-SA(1:2)	20	0.047	4.4	H_2O	100	4.0	72
5	TMDP-SA(1:2)	30	0.071	6.4	H_2O	100	4.0	72
6	**TMDP-SA(1:2)**	**20**	**0.047**	**4.4**	**H_2O**	**100**	**6.0**	**89**
7	TMDP-SA(1:2)	20	0.047	4.4	H_2O	100	8.0	89
8	TMDP-SA(1:2)	20	0.047	4.4	H_2O	80	6.0	68
9	**TMDP-SA(1:1)**	**20**	**0.065**	**5.9**	**HOAc**	**100**	**6.0**	**88**

[a] Reaction conditions: TCPB (1.03 mmol, 280 mg), Solvent (0.2 mL)
[b] GC yield
[c] The chosen optimal conditions.

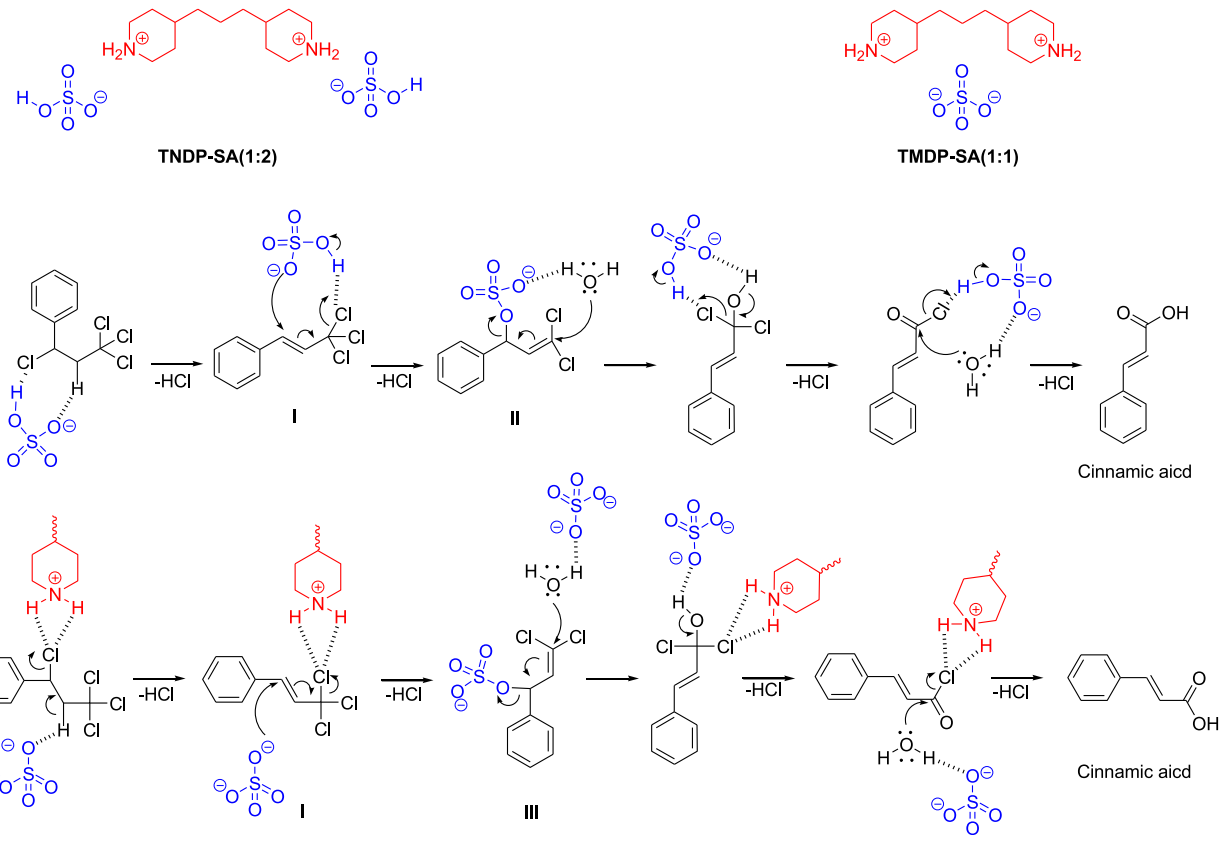

Scheme 2. A plausible scheme of the catalytic mechanism for the hydrolytic dehydrochlorination of 1,1,1,3-tetrachloro-3-phenylpropane in the presence of TMDP-SA(1:2) and TMDP-SA(1:1).

jugated 3-phenyl-1,1,1-trichloropropene as intermediate **I** through dehydrochlorination [51]. According to reported mechanisms in the literature, intermediate sulfate **II** or **III** are formed due to the electron-accepting property of the trichloromethyl group [52]. A direct nucleophilic attack of water on the α-carbon of the substrate displaces the chlorine atom with hydroxyl groups which gives cinnamic acid.

The reduction or elimination of corrosion plays a crucial role in the scale-up and industrial acetylation process. Therefore, a corrosive test was performed with TMDP-SA(1:2), TMDP-SA(1:1), and SA (98%) for a 316L austenitic stainless steel with length, width, and thickness of 50, 20, and 0.5 mm, respectively. The same amount of TMDP-SA(1:2) and SA (98%) (10 mg) was added into 100 mL of deionized water, and the stainless steel plates were put into the

Table 8
The recycling effect of TMDP-SA(1:2) on the conversion of the TCPB to cinnamic acid.[a]

Entry	Recycling	Yield (%)[b]
1	Fresh	89
2	1	89
3	2	88
4	3	87
5	4	87

[a] Reaction conditions: TCPB (1.03 mmol, 280 mg), water (0.2 mL), TMDP-SA (1:2) (20 mg, 4.4 mol%), temperature (100 °C), reaction time (6 h).
[b] GC yield

Table 9
Corrosive study of stainless steel by TMDP-SA(1:1), TMDP-SA(1:2), and SA (98%).[a]

Entry	The duration time (h)	Weight of stainless steel (g)		
		The solution of TMDP-SA(1:1)	The solution of TMDP-SA(1:2)	The solution of SA(98%)
1	-	3.9922	3.9923	3.9917
2	2	3.4922	3.2902	2.8012
3	8	3.3628	3.1635	1.3425
4	24	3.2916	3.1821	-

[a] Three stainless steel sheets were polished, cleaned, and dried to constant weight, then placed into the solution of TMDP-SA (1:1), TMDP-SA (1:2), and SA, respectively. After a mentioned time, two stainless steel sheets were pulled out carefully, washed in water, and dried and weighed.

solution. As one can see in Table 9, TMDP-SA(1:1) showed a much weaker corrosive property compared with TMDP-SA(1:2) and SA (98%), and the surface of stainless steel was intact even after 24 h.

3. Experiment

3.1. The synthesis of TMDP-SA(1:1) and TMDP-SA(1:2)

Initially, 4,4′-trimethylenedipiperidine (TMDP) (4.21 g, 20 mmol) was added into a bottom round flask containing dry CH_2Cl_2 (20 mL). After 10 min stirring at room temperature, the flask was taken into an ice bath. Then, SA (98%) (2.18 mL, ~40 mmol or 1.1 mL, ~20 mmol) was added dropwise into the solution. The mixture was stirred at an ice bath, then at room temperature overnight. The upper phase was decanted and the residue, viscous pale yellow liquids, was washed with CH_2Cl_2 (3 × 10 mL). The solvent was removed by a rotary evaporator. The colorless clear crystals were isolated in 94.8 and 96.2% yield for TMDP-SA(1:1) and TMDP-SA(1:2), respectively, from viscous liquids in methanol.

3.2. Synthesize of cinnamic acid through hydrolyzation of (1,3,3,3-tetrachloropropyl)benzene

The reactions were carried out in a round bottom flask capacity of 25 mL set in an oil bath and stirred with a magnetic stir bar at 400 rpm fitted with an exit glass tube. In a typical procedure, TCPB (0.5 mmol, 129 mg) was added to a solution of 50 mg of TMDP-SA(1:2) or TMDP-SA(1:1) in deionized water (1.0 mL), then the mixture was heated up to 100 °C and stirred for six hours. During the reaction, the hydrogen chloride vapor was transferred to a beaker containing deionized water by a glass tube, and the evolved HCl is absorbed by water. Due to the slight solubility of CA in water (0.5 g/1.0 L) and probably a leakage, the product was extracted by diethyl ether (3 × 2 mL). The residue was concentrated by a rotary evaporator. The recycled residue was used for the next run without any purification or washing.

Cinnamic acid: m.p. 131–132 °C, ^{1}H NMR (600 MHz, $CDCl_3$): δ 11.8 (br s, 1H, OH), 7.79 (d, 1H, J = 16.1), 7.51–7.54 (m, 2H, ArH), 7.35–7.45 (m, 3H, ArH), 6.45 (d, 1H, J = 16.1, CH=CH) ppm; ^{13}C NMR (150 MHz, $CDCl_3$): 172.7, 147.1, 134.0, 130.7, 128.9, 128.3, 117.3 ppm.

4. Conclusion

In conclusion, two novel acid salts containing two piperidinium rings linked by a three-carbon spacer and sulfate and hydrogen sulfate counterion were synthesized, and their chemical structures were elucidated by 1D and 2D NMR analysis. Further supports of the structure were obtained by the detailed FTIR and titrimetry analyses. Some physical properties and thermal behavior and thermal stability of the new acid salts were recorded and determined. The structure elucidation of TMDP-SA (1:2) showed that it is a diprotic acid like sulfuric acid, which can be used as a greener alternative to sulfuric acid. The catalytic activity of TMDP-SA (1:2) and TMDP-SA (1:1) was demonstrated to promote the hydrolytic conversion of (1,3,3,3-tetrachloropropyl)benzene to cinnamic acid under mild conditions. The present catalytic process has advantages such as simple experimental and sustainable procedure, high yield of the cinnamic acid, simple workup, and high recyclability of catalysts. Another superiority of the new method is avoiding a possible leakage of toxic heavy metals and heavy-metal waste generation.

Credit author statement

Lia Zaharani: Methodology, Investigation, Data curation, Formal analysis, Writing - review & editing.
Hayedeh Gorjian: Methodology, Investigation, Data curation.
Mohd Rafie Johan: Funding acquisition, Supervision.
Nader Ghaffari Khaligh: Conceptualization, Investigation, Data collection, Funding acquisition, Project administration, Resources, Supervision, Validation, Writing - original draft, Writing - review & editing.

Declaration of Competing Interest

authors declare that they have no known competing financial interests or personal relationships that could have appeared to influence the work reported in this paper.

Acknowledgments

This work was supported by a Research Grant (RU001-2020) for Scientific Research from the Universiti Malaya, Malaysia. The authors are thankful to staff members in the Analytical and Testing Center of Nanotechnology & Catalysis Research Center, the Universiti Malaya for partial support of this work.

Supplementary materials

Supplementary material associated with this article can be found, in the online version, at doi:10.1016/j.molstruc.2021.130977.

References

[1] R. K. Grasselli A. W. Sleight (Eds.) Structure-activity and selectivity relationships in heterogeneous catalysis (1st ed.), Elsevier Science, 1991, Vol. 67.
[2] L. Tušar, M. Novič, M. Tušar, J. Zupan, Structural elucidation, in: P. Worsfold, A. Townshend, C. Poole, M. Miró (Eds.), Chemistry, Molecular Sciences and Chemical Engineering. Encyclopedia of Analytical Science, 3rd ed., Elsevier Science, 2019, pp. 278–289.

[3] M.M. Martín, Sulfuric acidM.M. Martín (Ed.), Industrial Chemical Process Analysis and Design 7 (2016) 347–404 Ch, doi:10.1016/C2015-0-06319-5.
[4] H. Sharghi, P. Shiri, M. Aberi, An overview on recent advances in the synthesis of sulfonated organic materials, sulfonated silica materials, and sulfonated carbon materials and their catalytic applications in chemical processes, Beilstein J. Org. Chem. 14 (2018) 2745–2770, doi:10.3762/bjoc.14.253.
[5] A. Goeppert, P. Dinér, P. Ahlberg, J. Sommer, Methane activation and oxidation in sulfuric acid, Chemistry 8 (2002) 3277–3283, doi:10.1002/1521-3765(20020715)8:14⟨3277::AID-CHEM3277⟩3.0.CO;2-5.
[6] M. Belhouchet, M. Bahri, J.M. Savariault, T. Mhiri, Structural and vibrational study of a new organic hydrogen sulfate, Spectrochim. Acta A 61 (2005) 387–393, doi:10.1016/j.saa.2004.04.013.
[7] M.D. Lane, Mid-infrared emission spectroscopy of sulfate and sulfate-bearing minerals, Am. Mineral. 92 (2007) 1–18, doi:10.2138/am.2007.2170.
[8] F.A. Miller, C.H. Wilkins, Infrared spectra and characteristic frequencies of inorganic ions, Anal. Chem. 1952 (24) (1952) 1253–1294, doi:10.1021/ac60068a007.
[9] L. Zaharani, N.G. Khaligh, M.R. Johan, Synthesis, structure elucidation, vibrational and thermal behavior study of new one-core dication molten-salt, J. Mol. Struct. 1235 (2021) 130134, doi:10.1016/j.molstruc.2021.130134.
[10] A. Caraballo, S. Galán-Casado, Á. Caballero, S. Serena, Molten salts for sensible thermal energy storage: a review and an energy performance analysis, Energies 14 (2021) 1197, doi:10.3390/en14041197.
[11] W. Wang, Z. Wu, B. Li, B. Sundén, A review on molten-salt-based and ionic-liquid-based nanofluids for medium-to-high temperature heat transfer, J. Therm. Anal. Calorim. 136 (2019) 1037–1051, doi:10.1007/s10973-018-7765-y.
[12] L. Zaharani, N.G. Khaligh, M.R. Johan, H. Gorjian, Synthesis and characterization of a new acid molten salt and the study of its thermal behavior and catalytic activity in Fischer esterification, New Chem. J. 45 (2021) 7081–7088, doi:10.1039/D0NJ06273A.
[13] M. Yarie, M.A. Zolfigol, S. Babaee, S. Baghery, D.A. Alonso, A. Khoshnood, Catalytic application of a nano–molten salt catalyst in the synthesis of biological naphthoquinone–based compounds, Res. Chem. Intermed. 44 (2018) 2839–2852, doi:10.1007/s11164-018-3264-9.
[14] R.L. Vekariya, A review of ionic liquids: applications towards catalytic organic transformations, J. Mol. Liq. 227 (2017) 44–60, doi:10.1016/j.molliq.2016.11.123.
[15] T. Welton, Room-Temperature Ionic liquids. Solvents for synthesis and catalysis, Chem. Rev. 99 (1999) 2071–2084, doi:10.1021/cr980032t.
[16] G.W. Parshall, Catalysis in molten salt media, J. Am. Chem. Soc. 94 (1972) 8716–8719, doi:10.1021/ja00780a013.
[17] B.G. Swanson, in Encyclopedia of food sciences and nutrition (Second Edition), 2003
[18] P. De, M. Baltas, F. Bedos-Belval, Cinnamic acid derivatives as anticancer agents-A review, Curr. Org. Chem. 18 (2011) 1672–1703, doi:10.2174/092986711795471347.
[19] L.P. Zhang, Z.Z. Ji, Synthesis, anti-inflammatory and anticancer activity of cinnamic acids, their derivatives, and analogues, Acta Pharm. Sin. B. 27 (1992) 817–823.
[20] K. Zhou, D. Chen, B. Li, B. Zhang, F. Miao, L. Zhou, Bioactivity and structure-activity relationship of cinnamic acid esters and their derivatives as potential antifungal agents for plant protection, PLoS ONE 12 (2017) e0176189, doi:10.1371/journal.pone.0176189.
[21] M.A. Alam, N. Subhan, H. Hossain, M. Hossain, H.M. Reza, M.M. Rahman, M.O. Ullah, Hydroxycinnamic acid derivatives: a potential class of natural compounds for the management of lipid metabolism and obesity, Nutr. Metab. (Lond) 13 (2016) 27, doi:10.1186/s12986-016-0080-3.
[22] M. Bacanli, S.A. Dilsiz, N. Başaran, A.A. Başaran, Effects of phytochemicals against diabetes, Adv. Food Nutr. Res. 89 (2019) 209–238, doi:10.1016/bs.afnr.2019.02.006.
[23] A.C. Fonsec, M.S. Lima, A.F. Sousa, A.J. Silvestre, J.F.J. Coelho, A.C. Serra, Cinnamic acid derivatives as promising building blocks for advanced polymers: synthesis, properties and applications, Polym. Chem. 10 (2019) 1696–1723, doi:10.1039/C9PY00121B.
[24] A. Gunia-Krzyżak, K. Słoczyńska, J. Popiół, P. Koczurkiewicz, H. Marona, E. Pękala, Cinnamic acid derivatives in cosmetics: current use and future prospects, Inter. J. Cosmet. Sci. 40 (2018) 356–366, doi:10.1111/ics.12471.
[25] M. Hájek, P. Šilhav, US Pat., US 4,806,681, 1998; CA, 104; 186139w.
[26] C. Dai, J. Zhang, C. Huang, Z. Lei, Ionic liquids in selective oxidation: catalysts and solvents, Chemical Reviews 117 (2017) 6929–6983, doi:10.1021/acs.chemrev.7b00030.
[27] P. Wasserscheid, M. Sesing, W. Korth, Hydrogensulfate and tetrakis(hydrogensulfato)-borate ionic liquids: synthesis and catalytic application in highly Brønsted-acidic systems for Friedel-Crafts alkylation, Green Chem 4 (2002) 134–138, doi:10.1039/B109845B.
[28] X.S. Lin, Y. Zou, K.H. Zhao, T.X. Yang, P. Halling, Z. Yang, Tetraalkylammonium ionic liquids as dual solvents–catalysts for direct synthesis of sugar fatty acid esters, J. Surfact. Deterg. 19 (2016) 511–517, doi:10.1007/s11743-016-1798-7.
[29] D. Fang, X-L. Zhou, Z-W. Ye, Z-L. Liu, Brønsted acidic ionic liquids and their use as dual solvent-catalysts for Fischer esterifications, Ind. Eng. Chem. Res. 45 (2006) 7982–7984, doi:10.1021/ie060365d.
[30] A.C. Cole, J.L. Jensen, I. Ntai, K.L.T. Tran, K.J. Weaver, D.C. Forbes, J.H. Davis, Jr., Novel Brønsted acidic ionic liquids and their use as dual solvent-catalysts, J. Am. Chem. Soc. 124 (2002) 5962–5963, doi:10.1021/ja026290w.
[31] J. Shen, H. Wang, H. Liu, Y. Sun, Z. Liu, Bronsted acidic ionic liquid as dual catalyst and solvent for environmentally friendly synthesis of Chalcone, J. Mol. Catal. A Chem. 280 (2008) 24–28, doi:10.1016/j.molcata.2007.10.021.
[32] J. Weng, C. Wang, H. Li, Y. Wang, Novel quaternary ammonium ionic liquids and their use as dual solvent-catalysts in the hydrolytic reaction, Green Chem 8 (2006) 96–99, doi:10.1039/B508325G.
[33] N.G. Khaligh, T. Mihankhah, M.R. Johan, 4,4′-Trimethylenedipiperidine (TMDP): an efficient organocatalyst for the mechanosynthesis of pyrano[4,3-b]pyrans under solid-state conditions, Polycycl. Arom. Comp. 40 (2020) 1606–1615, doi:10.1080/10406638.2018.1564679.
[34] N.G. Khaligh, T. Mihankhah, M.R. Johan, Synthesis of new low-viscous sulfonic acid-functionalized ionic liquid and its application as a Brönsted liquid acid catalyst for the one-pot mechanosynthesis of 4H-pyrans through the ball milling process, J. Mol. Liq. 277 (2019) 794–804, doi:10.1016/j.molliq.2019.01.024.
[35] N.G. Khaligh, T. Mihankhah, M.R. Johan, An alternative, practical, and ecological protocol for synthesis of arylidene analogues of Meldrum's acid as useful intermediates, Res. Chem. Intermed. 45 (2019) 3291–3300, doi:10.1007/s11164-019-03796-2.
[36] L. Zaharani, N.G. Khaligh, M.R. Johan, H. Gorjian, Synthesis and characterization of a new acid molten salt and the study of its thermal behaviour and catalytic activity in Fischer esterification, New J. Chem. 45 (2021) 7081–7088, doi:10.1039/D0NJ06273A.
[37] K.M. Ward, R.S. Balaban, Determination of pH using water protons and chemical exchange dependent saturation transfer (CEST), Magn. Reson. Med. 44 (2000) 799–802, doi:10.1002/1522-2594(200011)44:5⟨799::AID-MRM18⟩3.0.CO;2-S.
[38] Atta-ur Rahman, Chemical Shifts and spin-spin couplings in ^{13}C-NMR spectroscopy, in: Nuclear Magnetic Resonance, Springer, New York, 1986, pp. 140–201, doi:10.1007/978-1-4612-4894-1_4.
[39] Y. Erdoğdu, M.T. Güllüoğlu, Ş. Yurdakul, Molecular structure and vibrational spectra of 1,3-bis(4-piperidyl)propane by quantum chemical calculations, J. Mol. Struct. 889 (2008) 361–370, doi:10.1016/j.molstruc.2008.02.019.
[40] T. Belhocine, S.A. Forsyth, H.Q.N. Gunaratne, M. Nieuwenhuyzen, P. Nockemann, A.V. Puga, K.R. Seddon, G. Srinivasan, K. Whiston, 3-Methylpiperidinium ionic liquids, Phys. Chem. Chem. Phys. 17 (2015) 10398–10416, doi:10.1039/C4CP05936K.
[41] H.D. Lutz, Structure and strength of hydrogen bonds in inorganic solids. J. Mol. Struct. 646 (2003) 227-236. https://doi.org/10.1016/S0022-2860(02)00716-0
[42] R.A. Heacock, L. Marion, The infrared spectra of secondary amines and their salts, Can. J. Chem. 34 (1956) 1782–1795, doi:10.1139/v56-231.
[43] H. Knorke, H. Li, Z-F. Liu, K.R. Asmis, Vibrational spectroscopy of the hexahydrated sulfate dianion revisited: role of isomers and anharmonicities, Phys. Chem. Chem. Phys. 21 (2019) 11651–11659, doi:10.1039/C9CP01802F.
[44] J. Baran, M.M. Ilczyszyn, M.K. Marchewka, H. Ratajczak, Vibrational studies of different modifications of the sodium hydrogen sulphate crystals, Spectrosc. Lett. 32 (1999) 83–102, doi:10.1080/00387019909349969.
[45] E.A. Secco, Spectroscopic properties of SO_4 (and OH) in different molecular and crystalline environments. I. Infrared spectra of $Cu_4(OH)_6SO_4$, $Cu_4(OH)_4SO_4$, and $Cu_3(OH)_4SO_4$, Can. J. Chem. 66 (1988) 329–336, doi:10.1139/v88-057.
[46] https://instanano.com/characterization/calculator/xrd/crystallite-size/
[47] https://instanano.com/characterization/calculator/xrd/d-value/
[48] M.S. Kharasch, E. Simon, W. Nudenberg, Reaction of atoms and free radicals in solution. XXIX. The relative reactivities of olefins toward the free trichloromethyl radical, J. Org. Chem. 18 (1953) 328–336, doi:10.1021/jo01131a017.
[49] M. Asscher, D. Vofsi, Chlorine activation by redox transfer. Part II. The addition of carbon tetrachloride to olefins, J. Chem. Soc. 1963 (1963) 1887–1896, doi:10.1039/jr9630001887.
[50] J. Weng, C. Wang, H. Li, Y. Wang, Novel quaternary ammonium ionic liquids and their use as dual solvent-catalysts in the hydrolytic reaction, Green Chem 8 (2006) 96–99, doi:10.1039/B508325G.
[51] H. Goldwhite, M.S. Gibson, C. Harris, Free radical addition reactions—II: the reaction of trichloromethanesulphonyl chloride with styrene, and chemistry of the adducts. Tetrahedron 20 (1964) 1649-1656. https://doi.org/10.1016/s0040-4020(01)99162-8
[52] R.K. Freidlina, V.N. Kost, A.N. Nesmeyanov, Action of chlorine on unsaturated polychloro compounds in an acid medium, Bull. Acad. Sci. USSR Div. Chem. Sci. 5 (1957) 1229–1234, doi:10.1007/bf01173780.